Modelling of Loss Factor Curves Obtained by Torsion-DMA of HTPB and GAP Based Binders manufactured with Different Curing Agents and Plasticizers

Tijen Seyidoglu and Manfred A. Bohn

Fraunhofer-Institute for Chemical Technology (ICT), D-76318 Pfinztal, Germany

Tijen.Seyidoglu@ict.fraunhofer.de

Manfred.Bohn@ict.fraunhofer.de

Abstract:

Inert non-polar HTPB binder and energetic GAP binder with polar groups are the two most common used binders to create a polymeric network for solid composite rocket propellant (SCRP) formulations. One of the key parameters during the development of a new SCRP formulation is the glass-rubber transition region, which is mainly dependent on the molecular interactions between the species and can be analysed using DMA loss factor (tanδ= G´´/G´) in torsion mode both for binders and highly filled SCRP. The current study aims to analyse the effect of different isocyanates and different plasticizers (inert & energetic) with HTPB R45HTLO and GAP based systems by tanδ curves applying BLC (baseline correction) and EMG (exponentially modified Gauss) distribution. GAP binders were prepared with Desmodur™ N100 and Desmodur™ N3400 types of curing agents and with three energetic plasticizers, Butyl-NENA, BDNPF/A and BATEG. The HTPB R45HTLO binders with four different types of isocyanates (IPDI, HDI, Desmodur™ E305 and 6HMDI), with and without the common plasticizer DOA (dioctyl adipate), were also analyzed using loss factor curves obtained by torsion DMA. The evolution of tanδ curves as a function of measurement temperature showed distinct differences in the intensity of loss factor curves with different isocyanates in the following order HDI > IPDI >> 6HMDI > DE305. Additional series of HTPB R45HTLO+IPDI binders with four different plasticizers (DOA, DOS, DOZ and IDP) showed not such pronounced differences compared with the differences obtained with the isocyanate types. Mainly, the four plasticizers showed the same level of intensity in loss factor curves and maximum peak temperature Tg, except IDP, which provided with the lowest glass-rubber transition temperature. Energetic plasticizer BATEG shifted the glass-rubber transition region tot lower temperatures; however, together with a lack of mechanical properties in terms of elongation. The isocyanate type changed the intensity of GAP binders. Comparing plasticizers BDNPF/A and Bu-NENA, the former provided better Tg.

Keywords: *HTPB binders; GAP based binders; curing agents, energetic and non-energetic plasticizers; DMA; loss factor; EMG modelling*

1 General Aspects

Design of a rocket propellant binder formulation requires certain points to consider in terms of glass-rubber transition, compatibility of the ingredients and mechanical properties. Due to the requirements during in-service applications, CRP binders with low glass-rubber transition (generally between -80°C and -70°C) and certain stress-strain capabilities are desired. Most properties of CRP depend on the mechanical strength of the binder network, which is mainly defined by the interactions of species, mainly polymer, plasticizer and curing agent present in the formulation.

Paper 118, pages 118-1 to 118-26 in Proc. of the 46th International Annual Conference of ICT on 'Energetic Materials – Performance, Safety and System Applications', June 23 to 26, 2015, Karlsruhe, Germany. ISSN 0722-4087. Fraunhofer-Institut fuer Chemische Technologie (ICT), D-76318 Pfinztal, Germany.

The current study aims to analyze the effects of different types of isocyanates and plasticizers with both HTPB and GAP based elastomeric binders to get a systematic overview in terms of loss factor curves that can be obtained by DMA. The shape and the position of the loss factor curve reflects information on glass-rubber transition regions and interactions of molecular structures present in the formulation.

2 Introduction

The binder pre-polymer named Glycidyl Azide Polymer (GAP) is one of the most interesting energetic binders and it is under concentrated exploration for gun and rocket propellants, gas generator systems and high explosives. The energetic properties of this binder originate from the azido groups, which decompose under combustion conditions to form nitrogen gas. They give the binder a higher energy content and a positive enthalpy of formation compared to HTPB binder propellants.

Conventional elastomeric binders of composite propellants consists of inert, non-polar HTPB as the polyol pre-polymer cross-linked by isocyanates to provide a suitable network for highly loaded (82 to 86 mass-% of solid fillers as Al and AP) propellant formulations and also in terms of processing and certain requirements for the final mechanical and thermal properties.

The glass-rubber transition temperature (T_g) of elastomer bonded composite rocket propellants is one of the key property determining their in-service functionality. DMA is a very suitable tool to analyze glass-rubber transition regions of the elastomeric systems through scanning the material from low to high temperature preferably at lower deformation frequencies. The loss factor (tanδ) curves obtained from DMA reveal the transition regions, which are affected by several factors: (1) filler type and content, (2) plasticizer type and content, (3) sterical hindrance, (4) interaction forces between all ingredients, (5) polymer chain conformation of the elastomer, (6) curing type and agent [1-2].

Suitable mathematical modelling of the loss factor curves of elastomeric networks and/or composite propellants enable to quantify different transitions regions in the polymeric networks and changes of these transitions with time allow to follow ageing. Because the loss factor region of most elastomers consists of several sub-transitions, a special modelling of the loss factor curve was developed using so named exponentially modified Gauss distributions (EMG) by Bohn and Cerri [1-6]. A separation of the molecular rearrangement regions or binder mobility fractions is achieved after the application of a suitable Base Line Correction (BLC) function to the loss factor curve. It was shown that DMA can be used as a further method besides other techniques such as tensile tests, sol-gel methods and GPC to follow the ageing of composite propellants [4-6]. Evaluation of change in the transition regions with time allows calculation of activation energy (E_a), which provides useful information in design of a new formulation and an ageing programme.

In the open literature, the effect of isocyanates in HTPB polymer network was investigated in different aspects, such as tensile properties [7,8], cure kinetics [9,10] swelling and solubility [8]. Effect of plasticizers in terms of tensile properties and of viscosity were investigated in [11]. Finding suitable plasticizer and cure system for GAP and ADN is still under investigation by many groups with different aspects but foremost in terms of high stress-strain capabilities [16-18]. In the current study, a set of different cure agents and plasticizers are chosen for HTPB and GAP polymeric binders and a systematic preview is provided by DMA tanδ curves to extract information on structure-property relationships of the species in the polymeric network.

3 Materials and experimental methods

3.1 Materials

Table 1 gives the properties of the materials used in the study. The ingredients were mixed in a remotely controlled planetary centrifugal vacuum mixer over the desired mixing time. The device is called Thinky Mixer™, type ARV-310 (distributing company in Germany: C3 Prozess-

und Analysentechnik GmbH, D-85540 Haar, Germany; the manufacturer is Thinky Corporation, 7F, Chiyoda-ku, Tokyo, Japan). The rotation speed was 1600 cycle per minutes and the pressure range 10 to 50 mbar. Table 2 shows the experimental parameters for the binder formulations; for GAP based samples similar conditions were used with different pauses in order to wait on the mix to cool down. Binder samples were cured in appropriate Teflon layered molds in electrical air flow oven cabinets (from company Memmert, Germany), standard curing was over five days at 60°C. The HTPB based binder formulations are given in Tables 3 to 4. The ratio of curing agent to polymer (Req = NCO/OH) or better the ratio NCO-groups to OH groups was adjusted to 0.869. GAP based binder formulations are given in Table 5. GAP binders were named with additional ´X´ to better distinguish them from the HTPB formulations. An equivalent ratio Req=1 was used for GAP based networks. Due to the hydrophilic nature of GAP itself and all three plasticizing energetics (Butyl-NENA, BDNPF/A and BATEG) they were dried in the rotary evaporator at least for 6 hours at 60°C at 100 mbar in a safety cabinet. Bu-NENA was stabilized with 0.5 mass-% 2-NDPA.

Table 1, Chemicals used in the study.

Trade Name	Supplier	Function	Properties
HTPB R45 HTLO	Sartomer, Polybd, Oakland USA	binder pre-polymer	OH = 0.83 (acetyl meq/g)
GAP	EURENCO, Paris, FR	binder pre-polymer	(Lot:06S12)
MW=2075 (1700-2300), MN=1904 (14002000), Polydispersity=1,09(≤1,3), OH Content=1220 (1000-1400),			
IPDI	Evonik, Marl, GE	curing Agent	MEQ = 111
HDI	Tramaco GmbH, Pinneberg, GE	curing Agent	MEQ = 84
6HMDI (=H12MDI)	Sigma-Aldrich, CAS:388386	curing Agent	MEQ = 131
Desmodur™ E305	Bayer MS, Leverkusen, GE	curing Agent	MEQ = 328
Vulkanox™-BKF	LANXESS, Leverkusen, GE	antioxidant	
DOA	BASF (Plastomoll DOA), GE	plasticizer	
IDP		plasticizer	
DOS (EDENOL 888) DOZ (EDENOL 9058)	Emery Oleochemicals GmbH, 40589 Düsseldorf, GE	plasticizer	
BDNPF/A	Dimension Technology Chemical Systems Inc., CA,USA	plasticizer	Lot:2S-176-139
BDNPA Content=%49,2 (45-55), BDNPF Content % 49,3 (45-55), Density, 25°C =1,396 g/cm^3 (1,383-1,397)			
BATEG	Produced in ICT	plasticizer	
Bu-NENA Butyl - *N* - (2 - nitroxyethyl) nitramine	Chemring Nobel AS	plasticizer	Density: 1,2 g/cm^3 Freezing point:(-27 °C) $T_{decompostion}$:210 °C

Table 2. Processing steps of formulations in Thinky Mixer™

Sequence of material addition	Mix Time	Vacuum Level
Polymer		
Vulkanox™ BKF	2 min	--
Plasticizer	2 min	30kPa
Cure agent	30 sec	--
	2 min	30kPa

Table 3. Binder formulations, concentrations in mass-%.

	TS-1	TS-4	TS-9	TS-11	TS-13	TS-16	TS-17	TS-20
HTPB R45 HTLO	90.70	67.15	69.25	59.56	92.32	68.02	89.53	79.42
IPDI	7.26					5.446		
6HMDI		6.34					8.46	

HDI			4.20		5.59			
E305				14.096				18.794
DOA		25	25	25		25.00		
Vulkanox™ BKF	2.042	1.51	1.56	1.34	2.08	1.53	2.02	1.79
Sum	100	100	100	100	100	100	100	100.00
Req (C/P)	0.869	0.869	0.869	0.869	0.869	0.869	0.87	0.869

Table 4. Binder formulations with different plasticizers, concentrations in mass-%-

	TS-29	TS-33	TS-34	TS-35
HTPB R45 HTLO	68.02	68.02	68.02	68.02
IPDI	5.45	5.45	5.45	5.45
IDP	25.00			
DOS (EDENOL 888)		25.00		
DOZ (EDENOL 9058)			25.00	
Vulkanox™ BKF (AOX)	1.53	1.53	1.53	1.53

Table 5. GAP Based Formulations

	TS-5XG	TS-7XG	TS-9XG	TS-11XG	TS-12XG	TS-14XG
GAP diol	73.39	73.49	64.756	64.848	80.41	64.848
Desmodur™ N3400	11.61		10.244			
Desmodur™ N100		11.51		10.152	12.59	10.152
Butyl-NENA			25	25		
BDNPF/A						25
BATEG	15	15			7	
Vulkanox™ BKF (AOX)						
SUM	100	100	100	100	100	100
EQ mass of curing agent	193	191	193	191	191	191
EQ mass of GAP	1220	1220	1220	1220	1220	1220

Table 6. Chemical Structures of Polyisocyanates.

Binder or Isocyanate Type	Chemical Structure
GAP	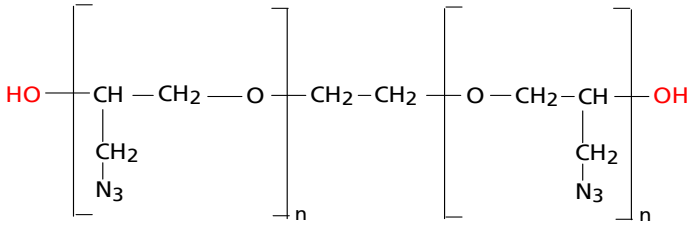
HTPB	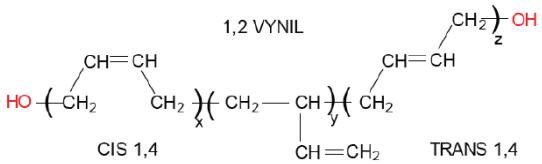
HDI	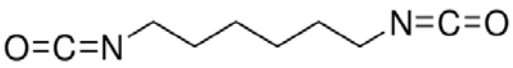
6HMDI (=H12MDI)	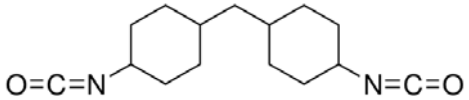

IPDI	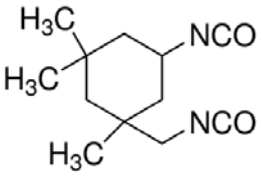
Desmodur™ N 100	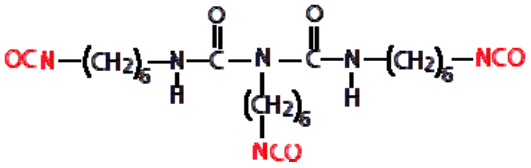
Desmodur™ 3400	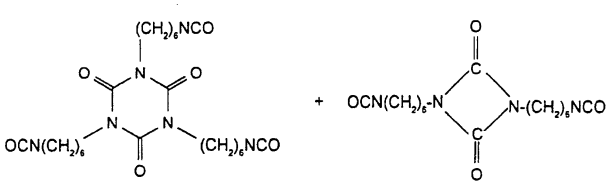 HDI trimer + HDI dimer

The structure of Desmodur™ E-305 is not communicated by the manufacturer. It is probably a condensation of a glycol and HDI.

Table 7. Structure of plasticizers used with HTPB

Plasticizer	Chemical Structure
DOA	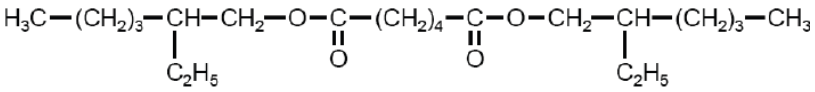
DOS	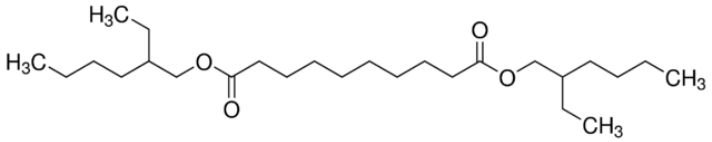
DOZ	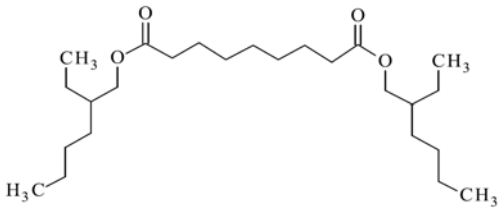
IDP	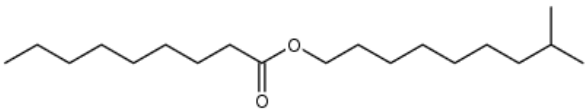

Table 8. Structure of energetic plasticizers used with GAP

Plasticizer	Chemical Structure
BDNPF / A bis dinitro propyl formal / acetal	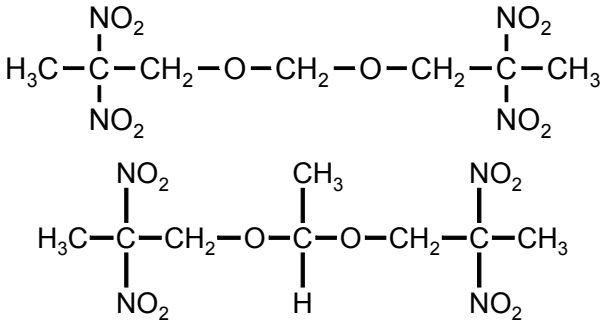
BATEG (bis-azido trtethylene glycol) 1,2-bis (2-azidoethoxy) ethane (also TEGDA).	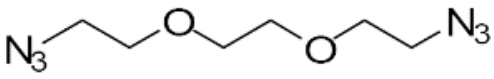
Butyl-NENA N-n-butyl-N-(2-nitroxy-ethyl) nitramine	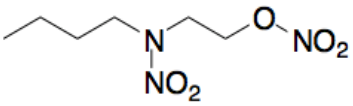

3.2 Measurements

3.2.1 DMA

All DMA measurements were carried out in torsion mode using a DMA instrument of type ARES^{TM} (Advanced Rheometric Expansion System) manufactured by former Rheometric Scientific Inc. (now belonging to Waters Inc., BU TA Instruments, Newcastle, Delaware, USA). Rectangular bars of about 10 mm wide, 4 to 5 mm thick, and 30 to 40 mm long were prepared for DMA. A liquid nitrogen cooling accessory was used for the low and high temperature operations. The investigated temperature range was -100°C to +70°C, with heating up in steps of 1 °C/min and a soak time of 28 s. Specimens were tested at four to five deformation frequencies (0.1, 1, 10, 30 and 56 Hz) using a strain control with maximum strain obtained from -100°C strain sweep experiment, in order to be in the linear range domain, which means the modulus is independent of strain. For some formulations, the (stepwise) temperature scan region was divided into 5 regions in which different strains were used, because of weakening of samples with increasing temperature.

3.2.2 Tensile Tests

The mechanical strength behavior of the formulations was characterized with a tensile test machine UPM 1476 from company Zwick / Roell, Ulm, Germany. Mini-dogbone samples were used in uniaxial tensile tests at room temperature and atmospheric pressure with a cross head speed (speed of traverse) of 50 mm/min. During each test the applied force and the elongation of the gauge length were recorded by a load cell and a mechanical extensometer, respectively.

3.2.3 DSC

Measurements were performed in nitrogen atmosphere using the DSC Q2000 manufactured by TA Instruments (Newcastle, Delaware, USA). Small amounts of propellants (about 10 mg) were analyzed between -100°C and ambient temperature with heating rate of 10 °C/min for determination of the glass-rubber temperature $T_{g,DSC}$ of the materials and the presence or absence of secondary relaxation phenomena.

4 Characterization of the HTPB type binders by DMA

4.1 Determination of loss factor curves

DMA measures the response of a material to a forced sinusoidal deformation. It is reproducible, as long as the material is in linear viscoelastic region. The measured quantity in the torsion mode, which was proven to be suitable configuration for HTPB based SCRPs, is the torque M, which allows the determination of storage (elastic) shear modulus (G´ [Pa], ability of the sample material to store energy elastically), and loss (viscous) shear modulus (G´´[Pa], energy dissipated by viscous dissipation such as heating due to the friction and internal motions). The ratio of the viscous to the elastic component of the complex shear modulus G*, namely G´´/G´, is defined as the loss tangent (tanδ); it is equivalent to the tangent of the phase angle δ between the applied strain and the torque response. It is regarded as an indicator of how efficiently the material loses energy to molecular rearrangements and internal friction and because it is independent of geometrical dimensions, it allows to get comparisons of different samples in a more confident way.

During a temperature scanning, an elastomeric binder or propellant (=elastomeric binder highly filled with energetic solid particles), faces a change from a glass-like to rubber-like behaviour by increasing temperature, where molecular rearrangements occur which reflect the molecular mobility of the polymeric networks during the glass-rubber transition. The necessity of applying a baseline correction (BLC) to the obtained raw data of tanδ is to get the correct areas under the loss factor curve, which are representing different mobility regions. The procedure is developed and explained in detail in the works of Cerri and Bohn [1, 4]. Following BLC, a suitable modelling function was used to quantify the different areas in tanδ curve. For this an exponentially modified Gauss function (EMG) is used, which is created by convolution of a Gaussian distribution function together with an exponential function given in Eq.(1). Molecular rearrangement regions are described by the Gaussian part of the EMG. By the exponential function the residual dissipative processes are considered as quasi-relaxation processes. The asymmetry of the EMG peak is determined by the ratio τ/w. Eq.(1) is adjusted to the baseline corrected data by non-linear fit algorithm with N equal to the numbers of extractable mobility regions. A Levenberg-Marquardt algorithm was used provided by the Origin™ program package [19].

$$\tan\delta = t_{d_0} + \sum_{i=0}^{N} \frac{A_i}{\tau_i} \cdot \frac{1}{2} \exp\left(0.5\left(\frac{w_i}{\tau_i}\right)^2 - \frac{T - Tc_i}{\tau_i} \right) \cdot \left\{ 1 - \mathrm{erf}\left(-\frac{1}{\sqrt{2}} \left(\frac{T - Tc_i}{w_i} - \frac{w_i}{\tau_i} \right) \right) \right\} \quad (1)$$

where,

T	measurement temperature [°C];
tanδ_BLC	value of the loss factor after the BLC as function of T [-];
A_i	peak areas of the EMG peaks, also equivalent to the area of the corresponding Gauss peak alone [°C];
w_i	half peak width at half height of only the Gaussian part [°C];
T_{ci}	temperature at peak maxima in the Gaussian part of EMG (not the peak maxima of EMG) [°C];
τ_i	relaxation parameter in exponential part of EMG [°C];
t_{d0}	residual offset in tanδ data [-], for evaluations here the value was fixed equal to 0;
N	number of EMG fit functions;
erf	error function

Figure 1 shows the storage modulus G´ and loss modulus G´´ of the HTPB binder prepared with HDI isocyanate obtained by DMA in torsion mode at three different deformation frequencies. In Figure 2 the loss factor curve of HTPB binder sample prepared with Desmodur™E305 can be seen. By scanning the sample with temperature, the tanδ curve reflects two main transition regions; the first one is located between -80°C to -60°C, whereas second one is broader than first one and appears between -20°C to +40°C. In the glassy state, at low temperature,

where the molecules are ‘bonded’ and narrowly aligned to each other, the behaviour of the tanδ is related to the changes in the elastic energy by small displacements of the molecules from their equilibrium positions. With increasing temperature the elastomeric material converts into the rubbery state, the material is expanded, the free volume increases so that localized chain movements and side chain movements can occur. The transition regions shift to higher temperatures with increasing strain rate or deformation frequency (strain rate hardening). These transition curves of the binders or filled elastomers reflect the nature and the restrictions exerted by the fillers on the polymeric network.

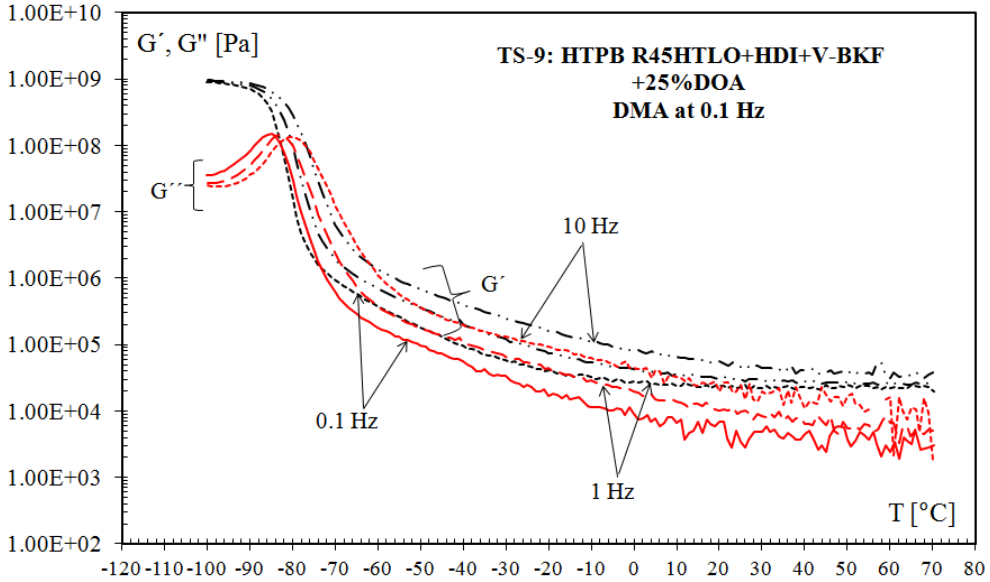

Figure 1. Storage shear modulus G´ and loss shear modulus G´´ of TS-9 vs. measured temperature at three different deformation frequencies.

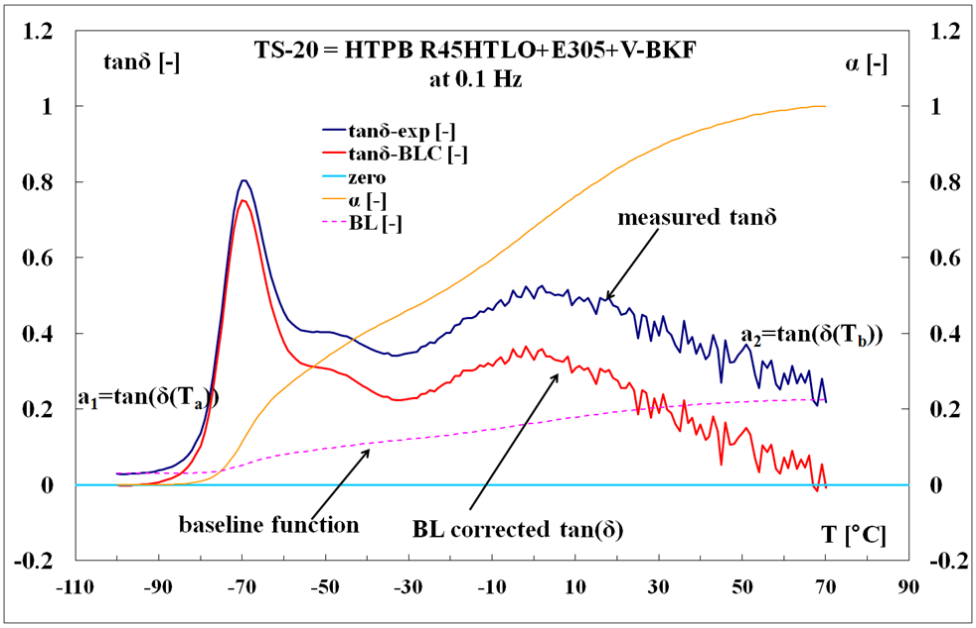

Figure 2: Application of BLC to tanδ data of binder TS-20 prepared with Desmodur™ E305

4.2 Effect of isocyanate types on loss factor in HTPB HTLO+V-BKF systems.

Baseline corrected tanδ curves of binders, formulated with four different types of isocyanates with and without plasticizer DOA are shown in Figures 3 and 4 respectively, at two deformation frequencies. Intensities of the tanδ curves change in the following order HDI > IPDI > 6HMDI > Desmodur™ E305 for both sets of binders with and without DOA. Same type of reorientations in the polymeric network are acting and increase the tanδ peak height and/or the area under the tanδ curve. A lower glass-rubber transition can be achieved by higher mobility of chain elements or structural elements of the polymeric chains (maximum temperature of corresponding tanδ curve).

Considering chain structures of the medium long chain aliphatic isocyanates, HDI has the highest intensity reflecting that HTPB network has less restrictions, in other words has more free volume compared to other isocyanate networks. Comparison of aliphatic IPDI with 6HMDI gives lower tanδ intensity with the latter. This can be explained by the structure of 6HMDI with its two relatively large cyclohexyl rings. These larger groups facilitate to hinder the polymer networks around the urethane cross-link. Further on, because of the more linear structure some H-bond interactions between the urethane groups are possible.

The network formed by IPDI, which has a rigid molecular ring and the two NCO groups not far away from each other, restricts the HTPB chain movements and this restriction is reflected in the reduced intensity of the tanδ curve compared to HDI. This less hindrance of HTPB chains by HDI also allows glass-rubber transition of the network to be at lower temperatures compared to IPDI. In other words, at low temperatures linear chain structure of HDI provides more free volume and helps the mobility of long chains of HTPB molecules.

The trend observed with different isocyanate types can also be linked to the Molar Refractivity, R, of the isocyanates which is a measure of the total polarizability of a mol of a substance and is dependent on the temperature, the index of refraction, and the pressure [20]. It is strongly related to the volume of the molecules and to London dispersive forces. The calculation of Molar Refractivity R is based on the atomic method proposed by Viswanadhan et al. [20]. 6HMDI (R =71.4) has the highest refractivity, then IPDI (R=59.25) and HDI (R=43.42) follow in decreasing order, which is parallel to tanδ intensities in reverse trend. (see Table 9) Taking into account this polarity values, one can conclude that molecular interactions, which hinders or restricts the polymer chains are highest with 6HMDI, IPDI and then HDI in the decreasing order. There is no definite structure available for Desmodur™-E305 supplied by the producer, except it is known that it is a linear aliphatic NCO pre-polymer based on HDI [21]. The molar refractivity R is related to the electronic polarizability α_e of a molecule. Assuming a sphere the relation is given in the following equation.

$$R = \frac{4}{3}\pi \cdot N_A \cdot \alpha_e \qquad (2)$$

Table 9. Correlation between molar refractivity R and the height of loss factor peak.

Isocyanate	Molar refractivity R [cm^3/mol]	Height of main peak in tanδ_BLC at 0.1 Hz
6HMDI	71.4	1.05
IPDI	59.25	1.18
HDI	43.42	1.42

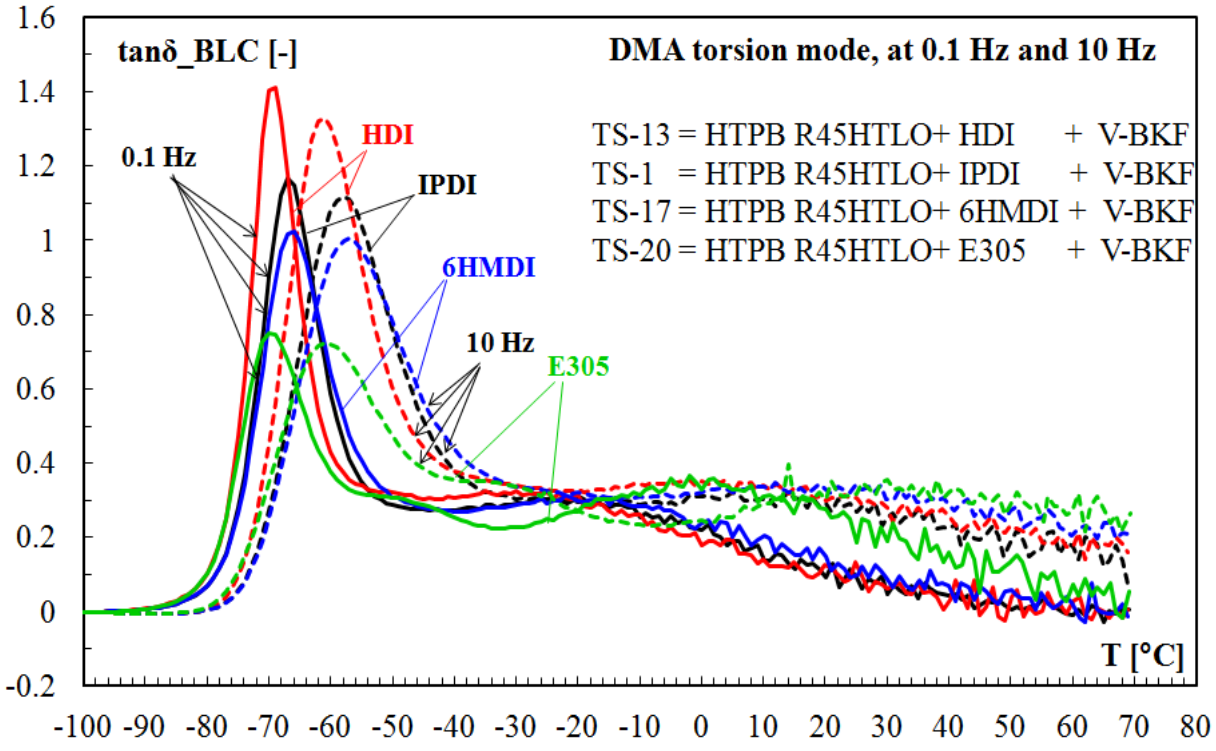

Figure 3. Base line corrected tanδ curves of TS-13, TS-1, TS-17 and TS-20 binders (without plasticizer DOA) vs. measured temperature at three different deformation frequencies.

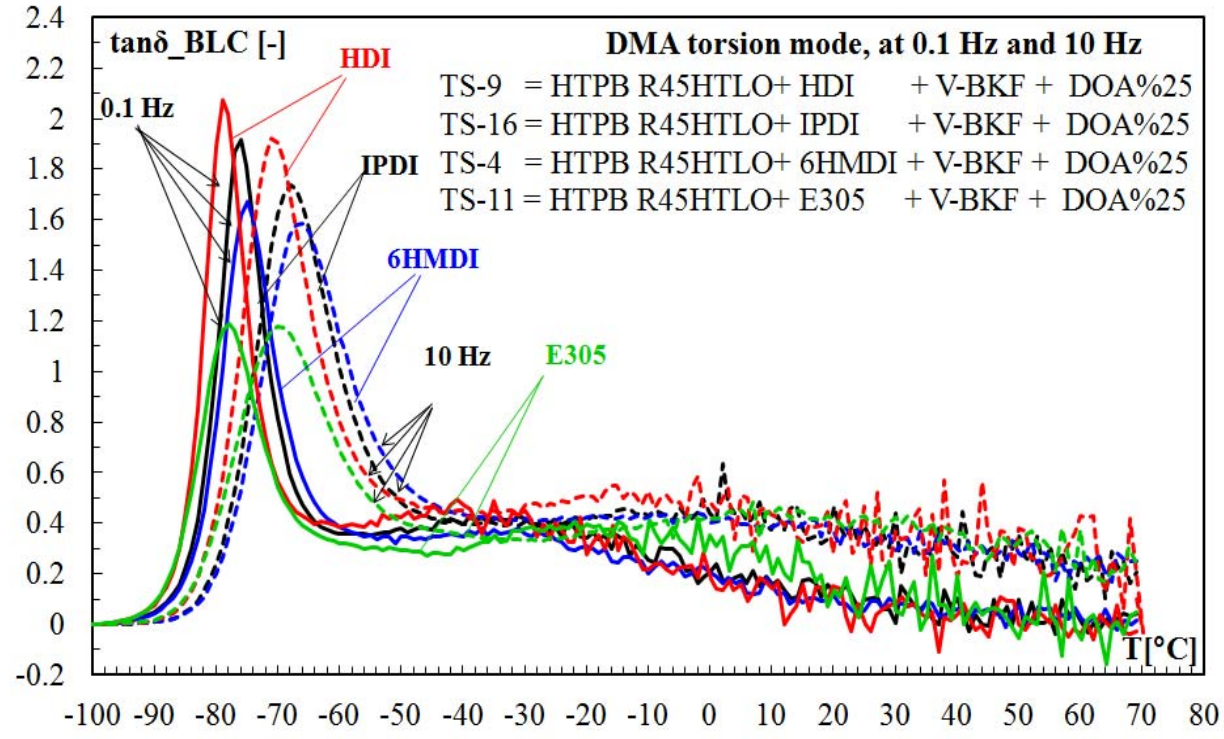

Figure 4. Base line corrected tanδ curves of TS-9, TS-16, TS-4 and TS-11 (with 25 mass-% plasticizer DOA) vs. measured temperature at three different deformation frequencies.

4.3 Glass-rubber transition temperatures by DMA and by DSC

The Tables 10 to 13 list the temperature in the main maxima of the T_{max}(tanδ_1) and the one of the loss modulus, T_{max}(G''). These temperatures can be taken for a parameterization of Arrhenius type with the deformation frequency according to Eq.(3).

$$f(T_{max}) = Z_f . \exp\left(-\frac{Ea_f^*}{R \cdot T_{max}} \right) \qquad (3)$$

Evaluated Arrhenius type apparent activation energies (Ea_f^*) from T_{max} (tanδ_1) of the loss factor and the temperature T_{max}(G´´) of the loss modulus G´´ are given in Table 11. The correlation (R^2) is good with all formulations. The first peak in G'' is related to the long chain interactions of HTPB polymer. There are a lot of interaction sites (here mainly of van-der-Waals type) resulting in the high activation energy to separate them. Further on, the temperature is already quite low and the distances between the molecules are quite small, which again increases the interaction energies. On the other hand the first maximum of loss factor appears at higher temperatures and the molecules are then already somewhat separated. The interaction energies are smaller and the resulting activation energy for shifting the maximum according to strain rate hardening is smaller [4]. The activation energies calculated from T_{max} in G´´ give much higher values, $Ea_f^*{}_{G''(Tmax)}$ ≈ 240-280 kJ/mol, compared the activation energies calculated from T_{max}(tanδ_1), i.e., $Ea_f^*{}_{tan\delta''(Tmax)}$ ≈ 160-180 kJ/mol.

DSC analysis provides information in terms of change in specific heat during a temperature scan as material experiences a transition from energy to entropy elasticity state. By this analysis the glass-rubber transition temperature $T_{g,\,DSC}$ can be identified as half height in the step of the specific heat change and it is always lower than the one obtained with DMA (Table 10 to 13). In DSC, the material does not experience a mechanical deformation, and thus it can be regarded as a static determination, neglecting the volume change by thermal expansion. As mechanical deformation rate (expressed by DMA deformation frequency) increases, it results a pseudo increase in strength by inertia effects inside the material. This leads to a shift of the transition region to higher temperatures. Figure 5 illustrates this case as T_{max} of tanδ shifts to higher temperatures as deformation frequency increases. Illustrative spoken the picture is that by increasing the deformation rate the material has less time to readapt the positions and orientations of the molecular groups and, coming from the low temperature side, the energy elastic behavior is remembered longer the higher the deformation rate is. Hence, DSC glass-rubber transition temperatures match to very low deformation rates in DMA. In order to compare Tg values from DSC and DMA the DMA deformation frequency should be chosen at 0.001Hz or smaller. Besides, DSC cannot provide information on the rearrangement processes, which are not accompanied by a change in specific heat of the network. DSC glass-rubber transition temperatures give much too low values with respect to application loads, which can have deformation rates up 1000 Hz and higher.

Table 10. Temperatures at maxima in loss factor, loss modulus of HTPB-IPDI.

Type of maximum temperature	T_{max} [°C]				
	0.1 Hz	1 Hz	10 Hz	30 Hz	$T_{g,DSC}$
	without DOA (TS-1)				
tanδ _max1	-66.94	-62.6	-57.75	-55.03	-73.92
G´´	-74.06	-71.41	-68.87	-66.93	
	with 25 mass-% DOA (TS-16)				
tanδ _max1	-76.36	-71.81	-67.16	-64.76	-84.08
G´´	-83.57	-80.58	-77.83	-76.17	

Table 11. Temperatures at maxima in loss factor, loss modulus of HTPB-HDI.

Type of maximum temperature	T_{max} [°C]				
	0.1 Hz	1 Hz	10 Hz	30 Hz	$Tg_{,DSC}$
	without DOA (TS-13)				
tanδ_max1	-69.54	-66.01	-60.62	-58.64	-75.91
G´´	-76.29	-73.55	-70.75	-68.95	
	with 25 mass-% DOA (TS-9)				
tanδ _max1	-78.88	-74.59	-69.93	-67.34	-85.25
G´´	-85.36	-82.73	-79.83	-78.59	

Table 12. Temperatures at maxima in loss factor, loss modulus of HTPB-6HMDI.

Type of maximum temperature	T_{max} [°C]				
	0.1 Hz	1 Hz	10 Hz	30 Hz	$T_{g,DSC}$
	without DOA (TS-17)				
tanδ _max1	-66.43	-62.11	-56.86	-54.08	-73.73
G´´	-74.29	-71.55	-68.57	-67.12	
	with 25 mass-% DOA (TS-4)				
tanδ _max1	-75.11	-71.17	-65.92	-63.3	-83.19
G´´	-82.78	-79.99	-77.22	-75.72	

Table 13. Temperatures at maxima in loss factor, loss modulus of HTPB-Desmodur™ E305.

Type of maximum temperature	T_{max} [°C]				
	0.1 Hz	1 Hz	10 Hz	30 Hz	$T_{g,DSC}$
	without DOA (TS-20)				
tanδ_max1	-69.71	-65.35	-60.32	-57.77	-76.90
G´´	-76.32	-74.21	-71.21	-69.74	
	with 25 mass-% DOA (TS-11)				
tanδ _max1	-78.27	-74.59	-69.13	-66.76	-86.68
G´´	-85.64	-82.88	-80.11	-78.45	

Table 14. Apparent activation energy (Ea_f*) from Arrhenius evaluation of the shift of the peak temperature of the loss factor (tanδ) and of G´´ with deformation frequency. The lg is the logarithm to base 10.

		T_{max} in tanδ_max1			T_{max} in G´´		
Isocyanate Type	Batch No	Ea_f* [kJ/mol]	lg(Z_f [Hz])	R^2	Ea_f* [kJ/mol]	lg(Z_f [Hz])	R^2
IPDI	TS-01	179.7	44.55	0.9989	278.6	72.123	0.9940
IPDI+DOA	TS-16	168.1	43.43	0.9999	242.3	65.748	0.9990
HDI	TS-13	184.2	46.32	0.9936	262.8	68.775	0.9910
HDI+DOA	TS-09	164.8	43.39	0.9993	253.8	69.604	0.9997
6HMDI	TS-17	173.6	42.87	0.9981	270.5	70.065	0.9998
6HMDI+DOA	TS-04	165.3	42.66	0.9964	253.9	68.68	0.9998
DE 305	TS-20	173.7	46.62	0.9993	284.4	74.55	0.9937
DE 305+DOA	TS-11	162.1	42.54	0.9943	243.2	66.76	0.9990

4.4 Effect of plasticizers on tanδ curve of HTPB based binders

Loss factor curves of binders with and without plasticizer are shown in Figure 5 for formulation prepared with HDI isocyanate. The tanδ curves of other binder formulations show similar trend, e.g., binders with plasticizer DOA has higher intensity compared the one without it. Binders without plasticizer have higher activation energy, see Table 14, which means in the absence of plasticizer, network can be regarded as compact, and the energetic interactions be-

tween the polymer chains are higher, in other words more energy is needed to disintegrate the system. The intensity of the loss factor curves increases as plasticizer reduces the interaction between polymer chains; which in turn increases the free volume and enables flexibility to the HTPB network and the glass-rubber transition temperature is lowered.

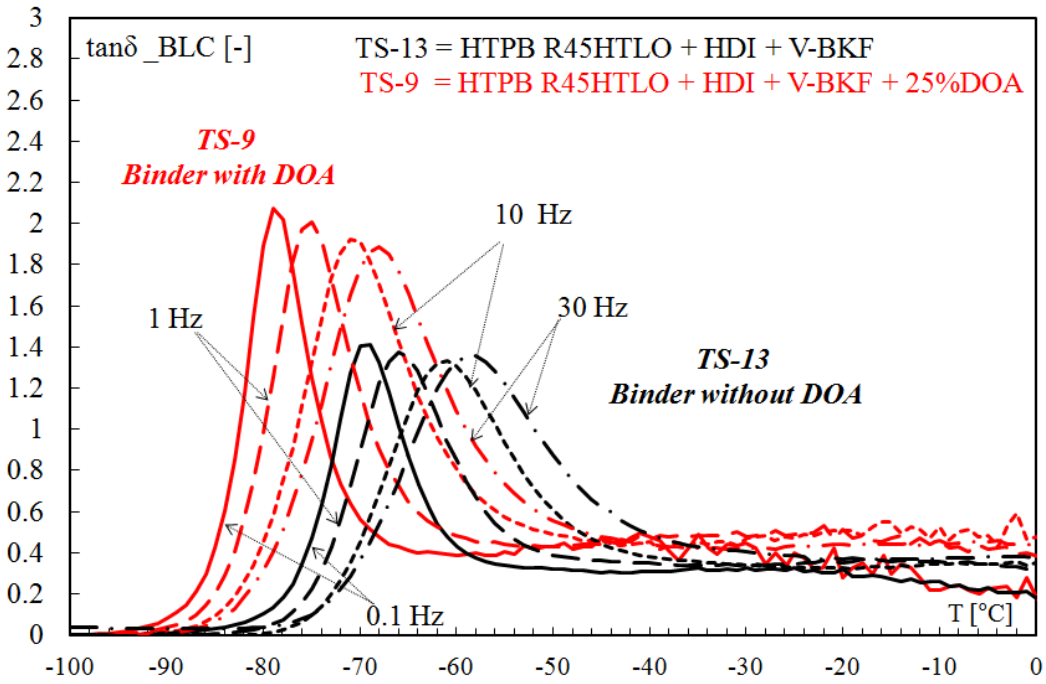

Figure 5. Effect of plasticizer DOA on the tanδ curves of binders prepared with HDI at three different frequencies. TS-9 contains 25 mass-% DOA.

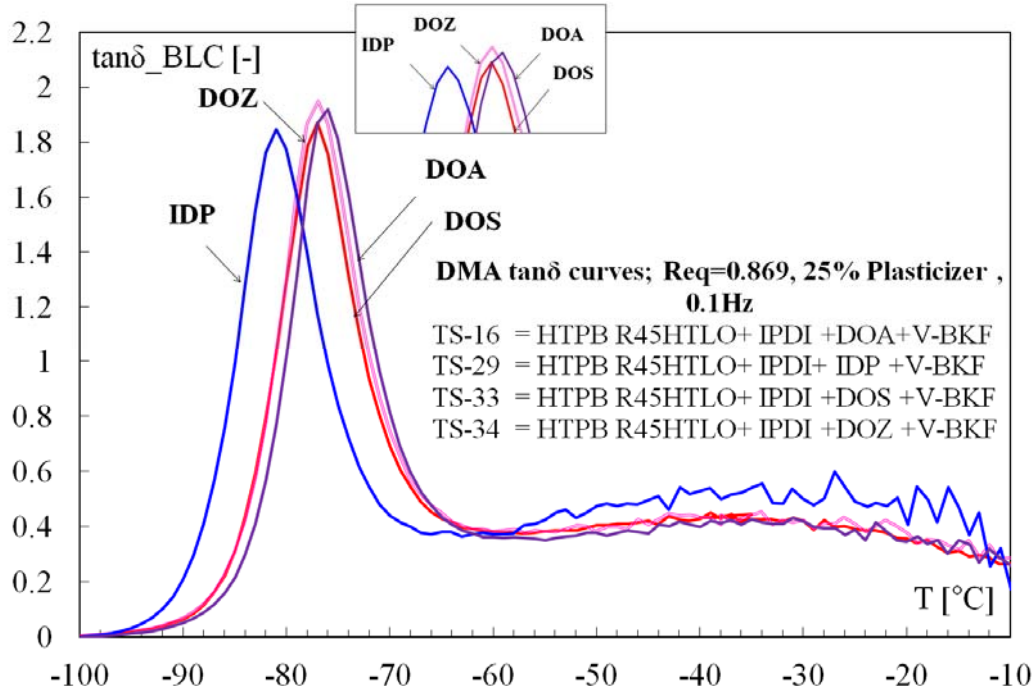

Figure 6. Effect of different plasticizers (always 25 mass-%) on DMA tanδ curve of HTPB based binder materials at 0.1 Hz

A plasticiser intrusion between the polymer chains decreases also the mobility restrictions caused by cross-linking sites, by opening the molecular arrangements. However, if geometrical hindrance around the curing agent occurs based on sterical conditions of chemical bonds and

atom arrangements, the plasticiser addition may not always remove this type of mobility restrictions. The restrictions are more pronounced in 6HMDI (=H12MDI) compared to IPDI and HDI isocyanates and the reason might be regarded as sterical hindrances by cyclohexyl rings and the dispersion interaction between the rings of two neighbouring 6HMDI groups together with H-bridge interaction between neighbouring urethane groups. These last two effects are especially pronounced with the MDI.

Comparison of DMA tanδ curves of four different plasticizers, DOA, IDP, DOS and DOZ are given in Figure 6. Formulations contain HTPB HTLO + IPDI + V-BKF and 25 mass-% of plasticizer. Considering the structures of four plasticizers, one can say they all have long chain structures and should be mostly compatible with HTPB-IPDI systems as the commonly used plasticizer DOA. Intensities at four different frequencies are close to each other. T_g of the sample with IDP is shifted to lower values compared to the effect of the other three plasticizers. Low T_g value with IDP may be explained by the low the molecular refractivity R of IDP (R=91.07); compared to other plasticizer with high value DOA (R=106.8); DOS (R=124.97); DOZ (R=120.6). As explained before, molecules, which can give more free volume to polymeric network due to fewer hindrances, in other words, which restricts the HTPB binder molecules less at low temperatures, give the lowest T_g as in the case of IDP.

4.5 Effect of isocyanates on tensile properties

Figure 7 shows the tensile test results of binders containing plasticizer obtained with minidogbone samples, using an extensometer to measure elongation. HDI and DE™305 with linear molecular structure gives better strain values compared to IPDI and the 6HMDI. Better performance of HDI and DE™305 can be explained by the medium long chains of HDI, which makes fewer restrictions on the HTPB networks as also observed in DMA analysis. In terms of maximum stress at break, 6HMDI has the highest value; but its strain capability is less than even with the common isocyanate IPDI. In the work of Nikolas et al. [7], high stress is also obtained with HMDI compared to IPDI and HDI. Nevertheless low strain capability of a binder network is not favourable considering long in-service time of a rocket propellant system. It is known that during ageing strain capability of a composite propellant decreases with time and up to a point it may reach a critical strain-stress level in that it cannot meet further requirements of safety concerns. DE™305 with its highest strain capability might be a candidate for substituting of IPDI. Stress values of E-305 binder might be increased with increasing Req value, since it still has high strain.

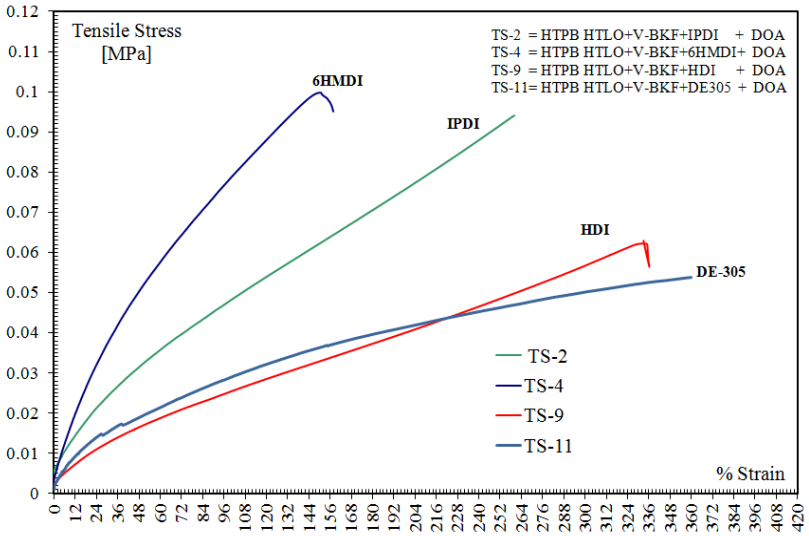

Figure 7. Tensile test results of binders prepared with 25 mass-% of plasticizer DOA

5 EMG Modelling of tanδ curves of HTPB formulations

5.1 Description of loss factor tanδ by exponentially modified Gauss distributions

EMG modelling enables to separate mobility ranges of binders with different fractions in order to quantify and to follow the changes with degree of rigid fillers bonded to the network and changes through aging of the elastomeric system. Figure 8 shows the description of tanδ curve of binder TS-11 prepared with Desmodur™ E305 and 25 mass-% DOA at 0.1 Hz. The use of two or three EMGs cannot describe the valley region very well between the apparent two peaks. Therefore N equal to 4 was used for TS-11. It shows a bending structure in the valley between first and second main peaks and the four EMGs defines the system well. The value of correlation coefficient R^2=0.96 might be considered well for the description of this special curvature. To fit four EMGs is not easy and may lead to numerical instabilities because of the error functions. Figure 9 shows the description of binder TS-1 with N=3 for HTPB+IPDI binder without DOA, which is very good.

The first peak in the tanδ curve is associated with long chain interactions of HTPB chains, there are more interaction sites (van-der-Waals type) giving the relatively high apparent energy to separate them. It mainly locates at about -78°C and belongs to glass-rubber transition of the main HTPB chain. The second transition around -25°C is assigned to short chain elements inside the rubbery shell and gives lower apparent interaction energies. With the binders prepared with IPDI, HDI and 6HMDI, with and without DOA, the EMG curves show similar trend in configuration of the curves, in other words two main transition regions. Quantitative description of the curves obtained by EMG function are given in Table 15. As said above Desmodur™ E305 shows more than three transition regions and was modelled with four EMG. The chemical structure of Desmodur™ E305 is not known except that it is a mainly linear NCO prepolymer based on hexamethylene diisocyanate (HDI) and has a polyether structure in between the isocyanate groups. EMG modelling enables one to calculate the area under the tanδ curves. Summation of the areas under the peak, A_1, A_2 and A_3 and A_4 are larger for samples prepared with DOA, which might be apparent also from the increase in the height of the peaks.

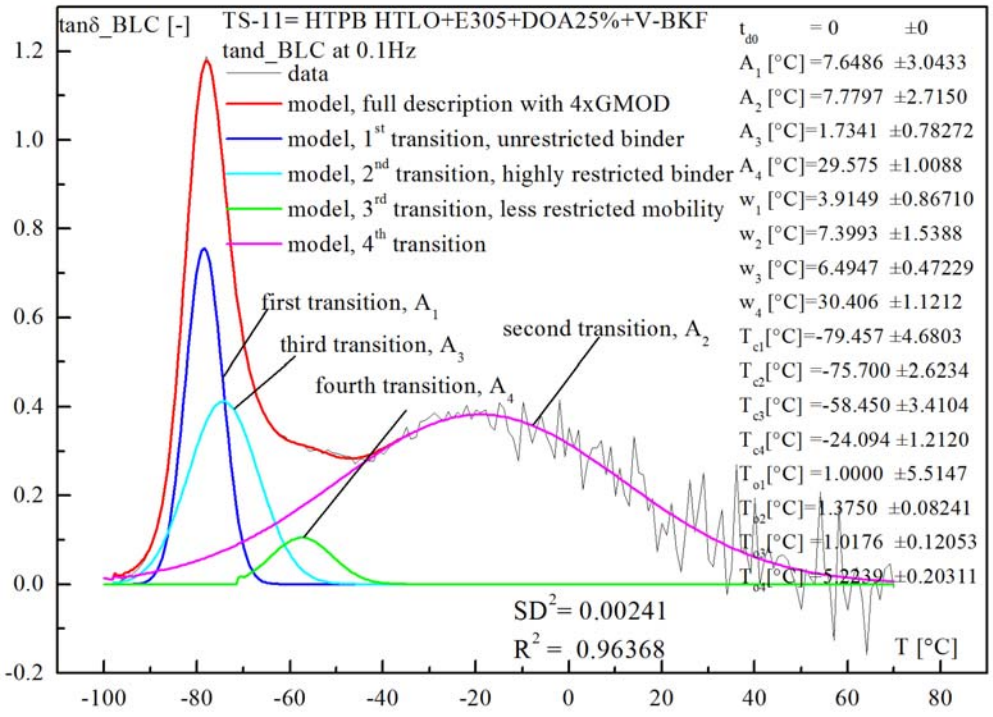

Figure 8: Description of the loss factor of the binder prepared with Desmodur™E305 with plasticizer DOA (25%) with 4xEMG (TS-11).

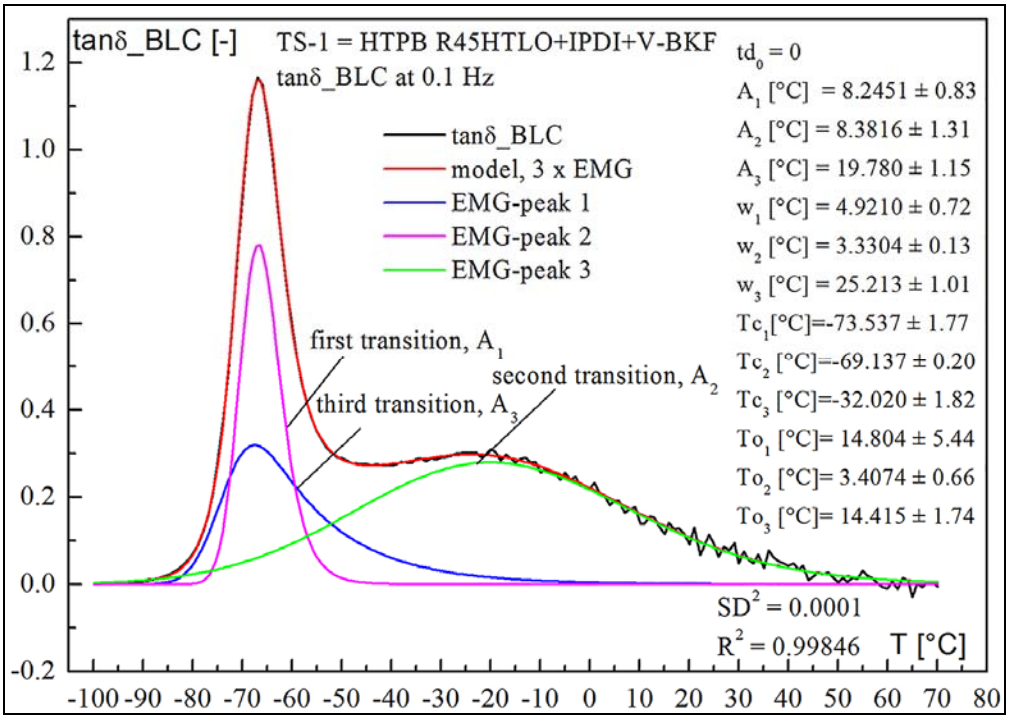

Figure 9. Description of the loss factor of the binder TS-1 prepared with HTPB R45HTLO with plasticizer DOA (25 mass-%) with 3 EMG functions,

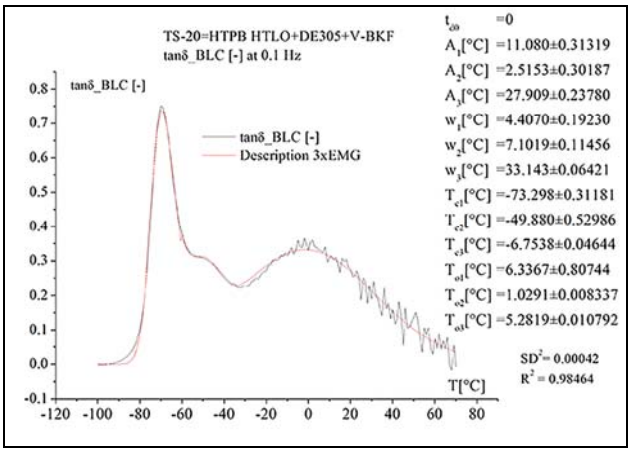

Figure 10. TS-20 binder HTPB - D E305; description of loss factor with 3xEMG.

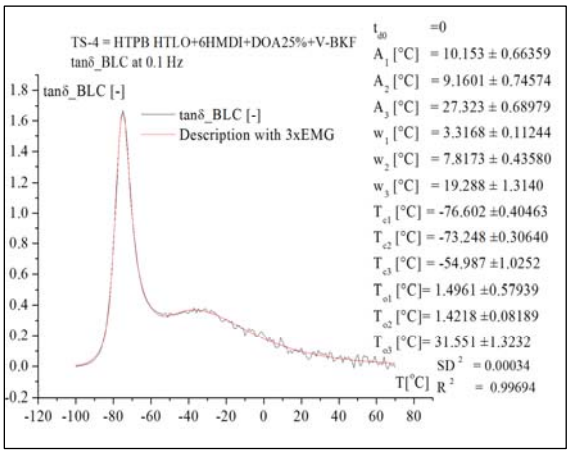

Figure 11. TS-4 binder HTPB - 6HMDI +DOA; description of loss factor with 3xEMG

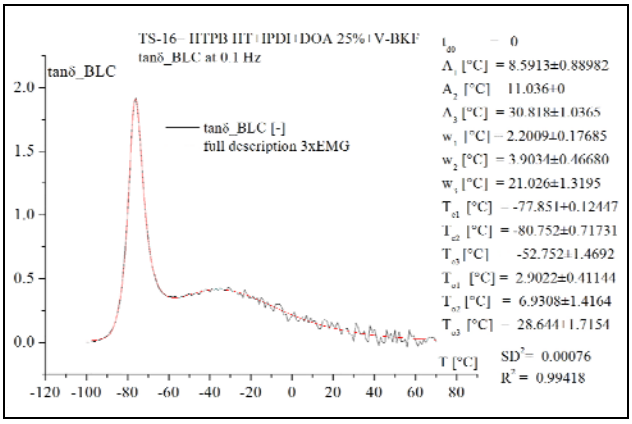

Figure 12. TS-13 binder HTPB - IPDI, description of the loss factor with 3xEMG.

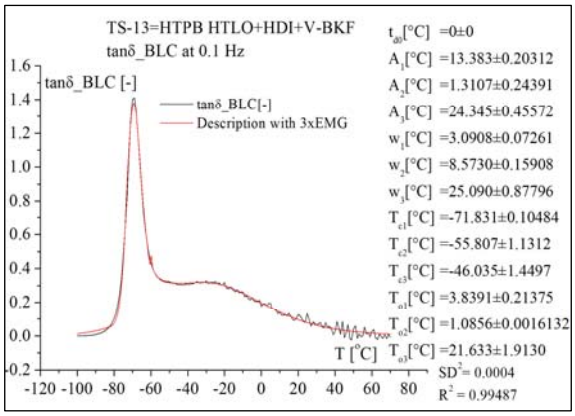

Figure 13. TS-13 binder HTPB -HDI, description of the loss factor with 3xEMG.

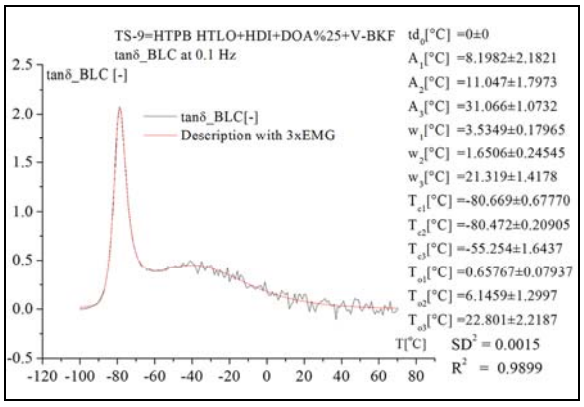

Figure 14. TS-9 binder HTPB - HDI+DOA, description of the loss factor with 3xEMG

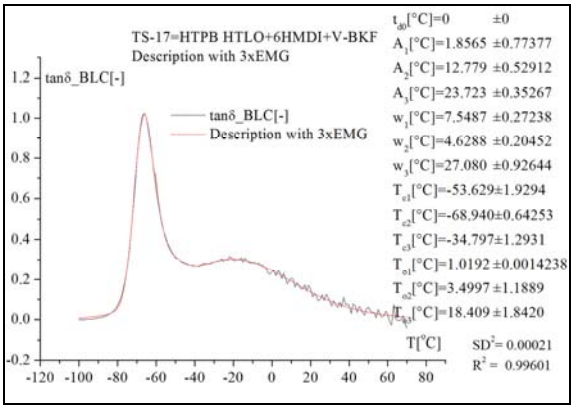

Figure 15. TS-17 binder HTPB - 6HDMI, description of the loss factor with 3xEMG

6 Energetic binders

A good plasticizer is physically compatible with polymer chains and improves its flexibility and glass transition properties. The energetic plasticizers should enhance flexibility and elasticity in addition to increase in the overall energy of a system and its burning properties. They regularly contain functional moieties such as nitrato, nitro, nitramine, fluoronitro, fluoroamino, azido etc. in addition to long carbon - carbon chains [10]. Here three different energetic plasticizers (Butyl-NENA, BATEG and BDNPF/A) with two different curing agents (Desmodur^{TM} N100 and Desmodur^{TM} N3400) were chosen to develop GAP based binder networks. For structures, see Tables 6 and 8.

Nitroxyethyl nitramine (NENA) plasticizers were originally discovered in the 1940s at the University of Toronto [23]. NENA´s contain both nitrate ester and nitramine functionalities and possess the general structure: RN (NO_2).CH_2 .CH_2.ONO_2 where R is methyl, ethyl, propyl, isopropyl, butyl and pentyl. Its most important contribution is regarded as provision of higher impetus compared to any other energetic ingredient [23]. Recent achievements on the use of Butyl-NENA plasticizer with GAP based composite propellants can be found in [16,18]. The study in [16] claims satisfactory tensile properties of a SCRP formulation produced with Bu-NENA and GAP based binders, meaning high elongation (25%) for GAP and ADN based propellants.

BDNP-F(formal)/-A(acetal) mixture was produced in USA during the development of polynitroaliphatic plasticizers in the late 1940s (because of their higher densities and higher oxygen content) in explosive and propellant formulations [24]. Nitroplasticizer containing equal amounts of acetal and formal, was more effective as a plasticizer rather than the individual compounds. This mixture is known to have good thermal and chemical stability, low hazard rating, convenience of handling and compatibility with propellant ingredients. The formal is a solid whereas the acetal is a liquid. Azido plasticizer triethylene glycol diazide (TEGDA) or BATEG (bis-azido triethelyene glycol) is another type of energetic plasticizer to be used in GAP binders. In order to have a satisfactory binder for solid propellant, GAP should be able to turn into a long-chain polyurethane with a correct curing agent. Especially to have a good level of mechanical properties such as strain, stress, and hardness levels, it is necessary to find the right curing agent. GAP is a quite linear molecule, only the typical bond angles give some bends. This leads to lower free volume around the main chain compared to HTPB and raises the glass-rubber transition temperature. It has strong polar groups (C-O-C and C-N-N-N) and permanent dipolar interchain interactions, and has relatively short average molecular chain length [2]. Glass-rubber transition of a binder is effected by the inter- and intramolecular forces between the polymer chains and plasticizers as well as between binder and filler particles.

Generally one can say that binder molecules without polar groups as C-O-C, C=O, C-OH, C-N have less interchain interaction energies than binder chains having such groups. HTPB with lower interaction energies provides higher free volume and glass-rubber transition region is at about -80°C while GAP with its strong intermolecular interaction gives a glass-rubber transition region between -50°C and -40°C:

Table 15. EMG modelling constants of the HTPB based binder formulations.

		TS-13	TS-9		TS-1	TS-16		TS-17	TS-4		TS-20	TS-11	TS-11
Isocyanate →		HDI			IPDI			6HMDI			D E305		
	unit	no DOA	with DOA		no DOA	with DOA		no DOA	with DOA		no DOA	with DOA	with DOA
N (number of EMG) →		**3**	**3**		**3**	**3**		**3**	**3**		**3**	**3**	**4**
t_{d0}	[°C]	0	0		0	0		0	0		0	0	0
A_1	[°C]	13.383	8.1982		8.2451	8.5913		1.8565	10.15		11.08	5.8031	7.65
A_2	[°C]	1.3107	11.047		8.3816	11.036		12.779	9.16		2.5153	13.601	7.780
A_3	[°C]	24.345	31.066		19.78	30.818		23.723	27.32		27.909	27.189	1.734
$\sum (A_1+A_2+A_3)$	[°C]	**39.038**	**50.311**		**36.406**	**50.445**		**38.359**	**46.64**		**-**	**-**	**46.74**
$\sum (A_1+A_2+A_3+A_4)$	[°C]	-	-		-	-		**-**	**-**		**41.50**	**46.59**	**63.90**
w_1	[°C]	3.0908	3.5349		4.921	2.2009		7.5487	3.3168		4.407	3.4115	3.9149
w_2	[°C]	8.573	1.6506		3.3304	3.9034		4.6288	7.8173		7.1019	4.878	7.3993
w_3	[°C]	25.09	21.319		25.213	21.026		27.08	19.288		33.143	28.229	7.3993
w_4	[°C]	-	-		-	-		-	-		-	-	30.406
T_{c1}	[°C]	-71.831	-80.669		-73.537	-77.851		-53.629	-76.602		-73.298	-79.727	-79.45
T_{c2}	[°C]	-55.807	-80.472		-69.137	-80.752		-68.94	-73.248		-49.88	-83.179	-75.70
T_{c3}	[°C]	-46.035	-55.254		-32.02	-52.752		-34.797	-54.987		-6.754	-24.551	-58.45
T_{c4}	[°C]	-	-		-	-		-	-		-	-	-24.09
T_{o1}	[°C]	3.8391	0.6576		14.804	2.9022		1.0192	1.4961		6.3367	1.9004	1
T_{o2}	[°C]	1.0856	6.1459		3.4074	6.9308		3.4997	1.4218		1.0291	14.275	1.375
T_{o3}	[°C]	21.633	22.801		14.415	28.644		18.409	31.551		5.2819	8.7977	1.0176
T_{o4}	[°C]	-	-		-	-		-	-		-	-	5.223
SD^2	[-]	0.0004	0.0015		0.0001	0.00076		0.00021	0.00034		0.00042	0.00237	0.0024
R^2	[-]	0.9949	0.9899		0.9985	0.9942		0.9960	0.9969		0.9846	0.9634	0.9637

7 Loss factor curves of GAP based binders

Corrected (BLC) data of tanδ from all GAP based binders at 0.1 Hz are given in Figure 16. GAP based binders shows mainly only one apparent peak, and a tendency to tailing towards the high temperatures, which is pronounced with formulations prepared with Bu-NENA. This type of behaviour differ from the one obtained with HTPB+isocyanate binders given in the previous sections. High free volume provided by long chains of HTPB shifts the glass transition to lower temperatures and molecular motions of hard segment units can be observed as a second transition. Peak separation provided in EMG modelling enables to highlight a second hidden transition in GAP based binders.

Figure 17 shows the comparison of the tanδ_BLC data of GAP based binders prepared with Bu-NENA and two different curing agents D-N100 (TS-11XG) and D-N3400 (TS-9XG). Similar set of binders prepared with BATEG and the same two curing agents (N100 in TS-7XG) (N3400 in TS-5XG) are given in the same figure, which allows comparison of the two cure agents. Here a further point to consider is the content of the plasticizer: BATEG content is 15 mass-% whereas Bu-NENA was used with 25 mass-%. The content of 15 mass-% of BATEG has already a brittle structure with GAP system. Although results are not given here samples with BATEG resulted in 20% elongation which may be regarded as a low value for a binder network, especially comparing to HTPB based binders with elongation of the order of 200-300%.

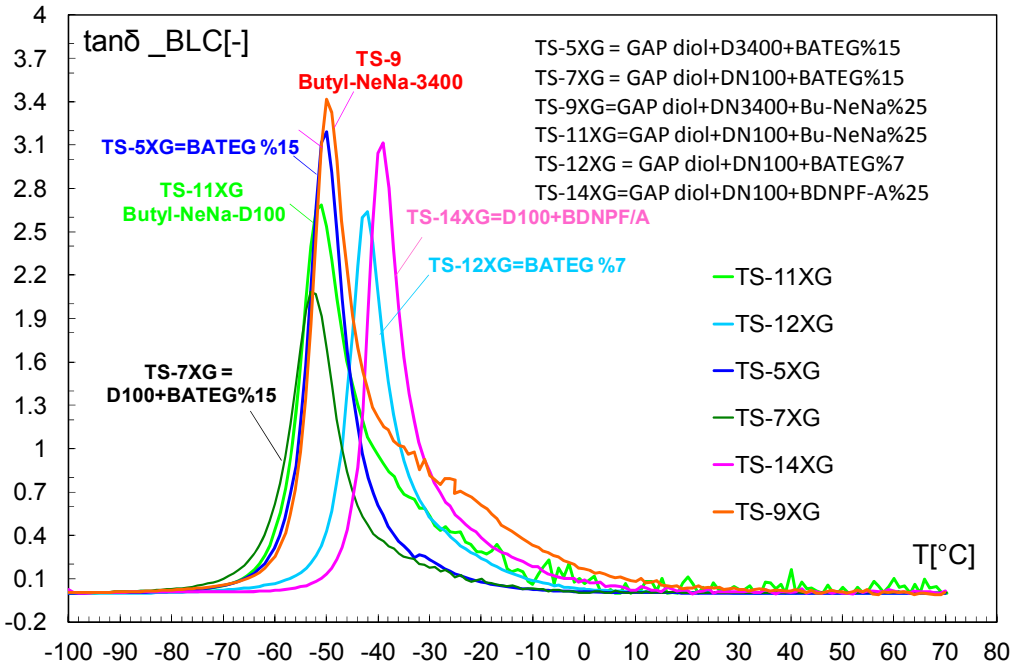

Figure 16. Comparison of all tanδ_BLC curves of the GAP formulations obtained with DMA in torsion mode at 0.1 Hz.

In an idealized linear thermoplastic polyurethane formation, one equivalent of long chain diol, one equivalent of short chain diol and two equivalents of di-isocyanate form the network given in Figure 18. The symmetry of the isocyanates and the nature of the chain extenders determines the interaction between different hard segments, which influence the possibility to form highly organized structures [24]. The long chain polyols, which are flexible and are usually entangled, relocate along the polymer chain with oligomeric rigid urethane units (hard segments). With D-N3400, aliphatic structures may provide higher free volume meaning more molecular level mobility to the GAP network and so the intensity of tanδ increases with the use of it. High intensity of tanδ provided with D-N3400 reflects more molecular flexibility and mobility compared to D-N100 recognizable with both plasticizers BATEG and Bu-NENA.

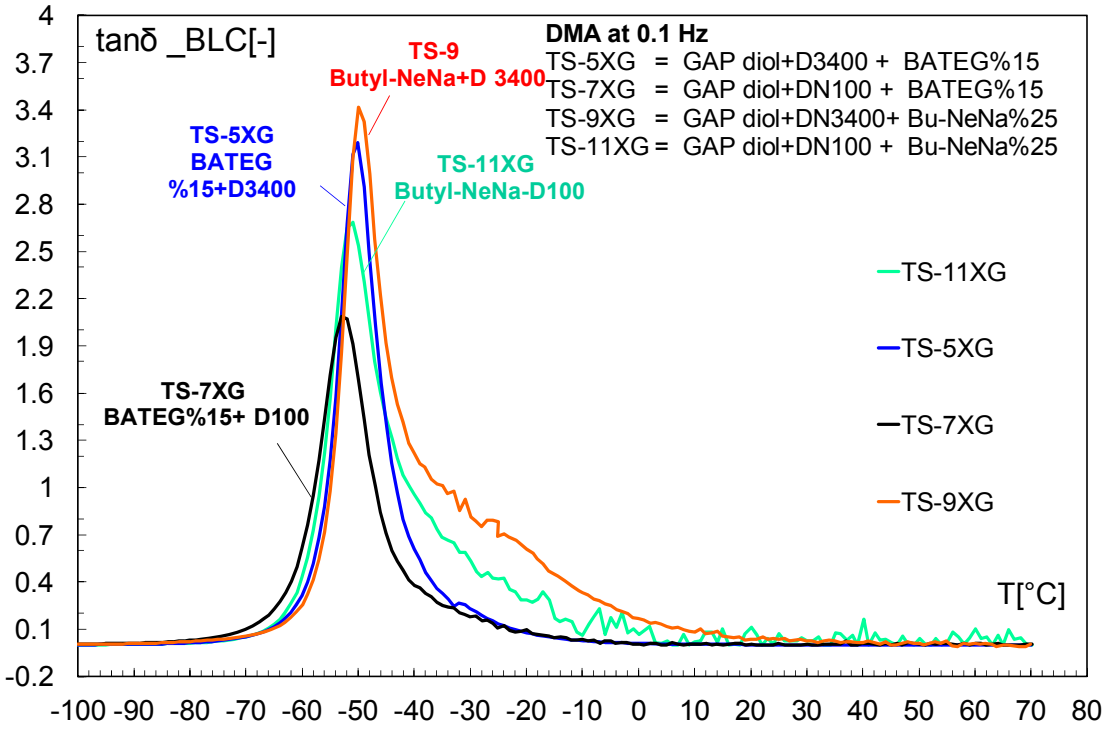

Figure 17. Comparison of tanδ_BLC curves of the GAP based binders prepared with Desmodur N100 and Desmodur N3400 (deformation frequency 0.1 Hz).

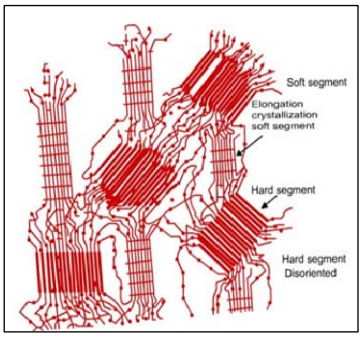

(a) Schematic representing of hard and soft segments in a thermoplastic elastomer [23]

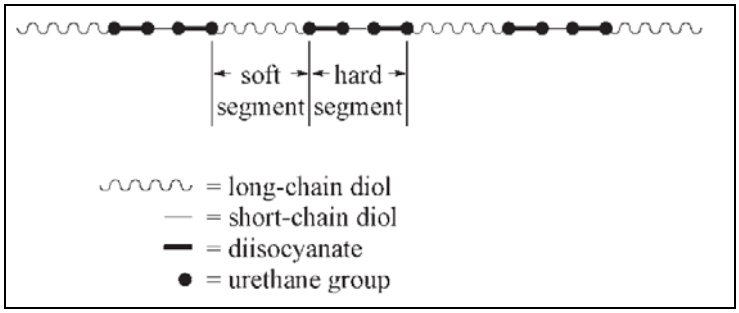

(b) Schematic primary structure of a segmented linear polyurethane chain [24]

Figure 18. Polyurethane network formation for thermoplastic linear PUR.

Figure 19 shows the GAP based binders prepared with curing agent D-N100. In terms of glass-rubber transition, BATEG is favourable compared to Bu-NENA and BDNPF/A as it shows already a lower transition region at 15 mass-%. However, mechanical properties of the binder with BATEG was not sufficient as mentioned already above. Comparison of BDNPF/A and Bu-NENA favours Bu-NENA in terms of glass-rubber transition. Bu-NENA with its linear, non polar chain structure in n-butyl and low molecular mass (MW=207g/mol) may be regarded as more compatible and effective with GAP than BDNPF/A (MW=319 g/mol) plasticizer. Nevertheless, molecular hindrance is less with BDNPF/A mixture as it shows higher intensity in tanδ. Flexible groups present in Bu-NENA such as n-butyl enhances the formation of free volume and therefore the main.chain flexibility of GAP and reduce the glass-rubber transition temperature [25]. Increasing BATEG content from 7 to 15 mass-% (TS-12XG and TS-7XG) caused a decrease in T_g of the GAP based binders. This can be explained as the general plasticizer effect in polymeric binders.

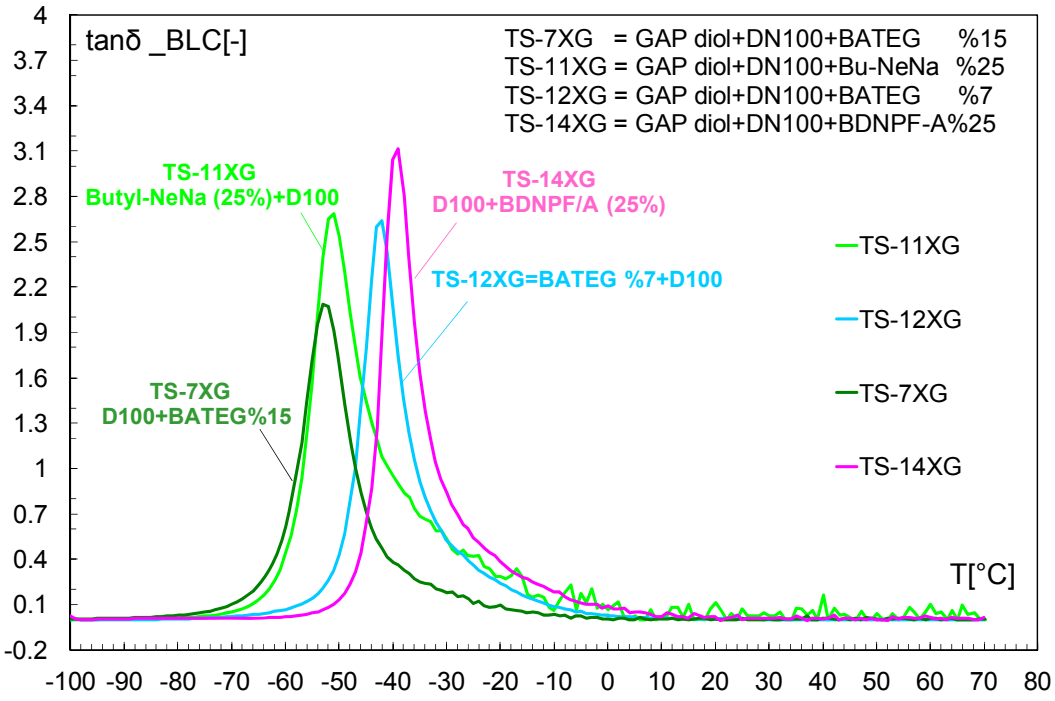

Figure 19. tanδ_BLC of GAP binders prepared with D-100.

The Table 16 list the temperature in the main maxima of the, T_{max}(tanδ_1) at four different frequencies and also Tg measured with DSC. Considering all GAP based formulations; BATEG seems to be more effective with GAP in terms of glass-rubber transition values. Evaluated Arrhenius type apparent activation energies (Ea_f*) from T_{max} (tanδ_1) of the loss factor are given in Table 17.

Table 16. T_{max} in tanδ curves and comparison with $T_{g,DSC}$

Maximum Type	T_{max} [°C]				
	0.1 Hz	**1 Hz**	**10 Hz**	**30 Hz**	**$T_{g,DSC}$**
	TS-5XG				
tanδ _max1	-50.15	-46.51	-41.48	-38.51	-56.50
	TS-7XG				
tanδ _max1	-52.3	-48.85	-43.97	-41.18	-63.92
	TS-11XG				
tanδ _max1	-50.35	-46.51	-41.91	-39.45	-57.19
	TS-12XG				
tanδ _max1	-42.06	-38.44	-33.65	-31.15	-48.46
	TS-9XG				
tanδ _max1	-49.81	-46.12	-41.75	-39.49	-56.01
	TS-14XG				
tanδ _max1	-39.14	-36.13	-31.6	-29.29	-44.09

Table 17. Arrhenius parameters from deformation frequency parameterization for GAP based binder systems. The lg is logarithm to base 10.

Content	Batch No	Ea_f* [kJ/mol]	lg(Z_f [Hz])	R^2
BATEG (%15) +D-3400	TS-5XG	212.30	48.754	0.992
BATEG (%15) + D-100	TS-7XG	216.75	50.356	0.9918
Bu-NENA + D-3400	TS-9XG	239.23	54.986	0.9841
Bu-NENA + D-100	TS-11XG	226.20	52.072	0.9998
BATEG (%7) + D-100	TS-12XG	241.26	53.601	0.9957
BDNPF/A + D-100	TS-14XG	270.29	59.429	0.9913

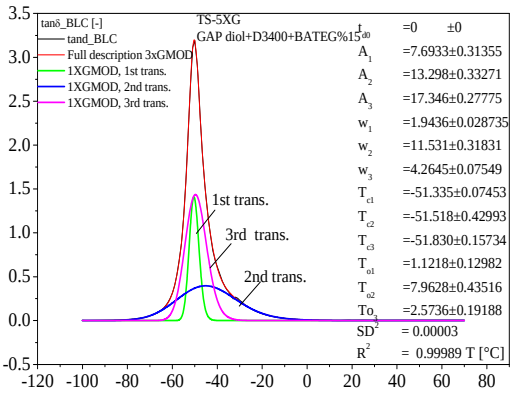

Figure 20. EMG of TS-5XG at 0.1 Hz

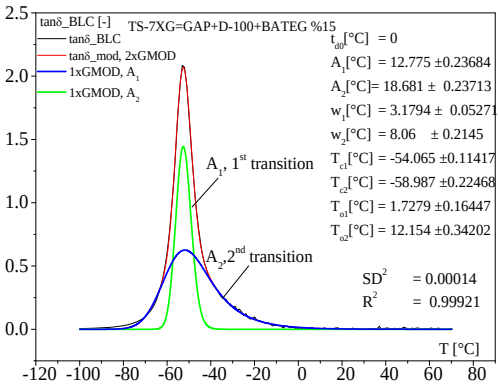

Figure 21. EMG of TS-7XG at 0.1 Hz

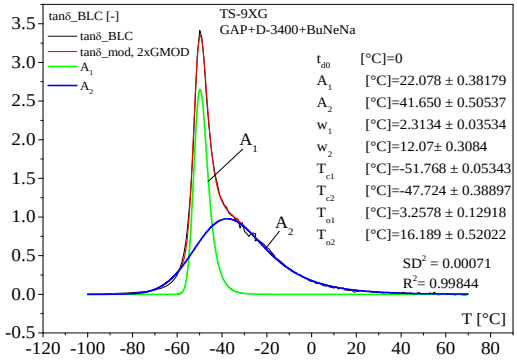

Figure 22. EMG of TS-9XG at 0.1 Hz

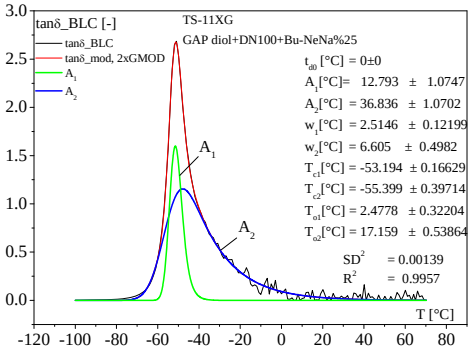

Figure 23. EMG of TS-11XG at 0.1 Hz

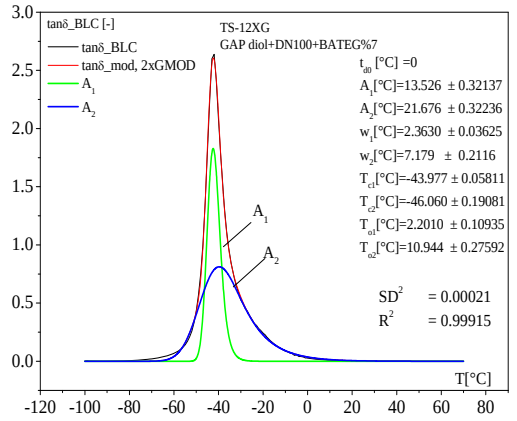

Figure 24. EMG of TS-12XG at 0.1 Hz

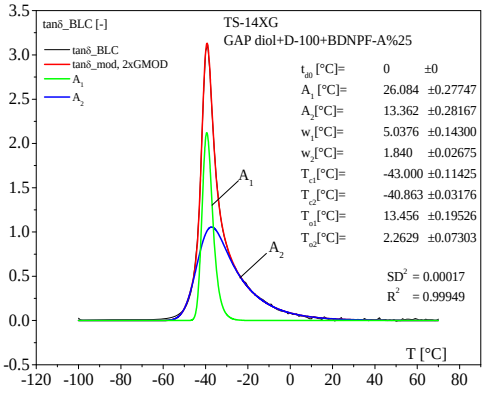

Figure 25. EMG of TS-14XG at 0.1 Hz

Figure 20 to 25 shows EMG modelled tanδ_BLC of GAP based binders with N=2. The number of fit parameters is equal to N*4, where N is the number of EMGs and 4 is the number of parameters per EMG: A_i, w_i, T_{ci} and T_{oi}. Considering N=2, 8 parameters can be evaluated. In the case of TS-5XG, data was modelled with N=3 as fitting with N=2 gives not in a good description level. tanδ of GAP based binders show asymmetry in the curve and a tail through the high temperature side and differs to the ones obtained with HTPB network. Similar behaviour of GAP based propellant formulations produced with ADN was shown in [26]. Binders with GAP have no two apparent peaks as with HTPB. But a peak separation enables to see the hidden second peak in the formulations, which is not directly observable from the total shape of the curve. Table 18 summarizes the EMG model fitting constants evaluated for the corresponding BLC data of the formulations. Sum of transitions areas (A_1+A_2+A_3) is highest with TS-9XG which is also detectable from the intensity of the tanδ curves.

Table 18. EMG modelling constants of the GAP based binder formulations.

		TS-5XG	**TS-7XG**	**TS-9XG**	**TS-11XG**	**TS-12XG**	**TS-14XG**
Curing agent →		N3400	N100	N3400	N100	N100	N100
Energetic plasticizer		*BATEG*	*BATEG*	*Bu-NENA*	*Bu-NENA*	*BATEG*	*BDNPF/A*
Plasticizer mass-%		15	15	25	25	7	25
	unit						
N (number of EMG) →		3	2	2	2	2	2
t_{d0}	[°C]	0	0	0	0	0	0
A_1	[°C]	7.6933	12.775	22.078	12.793	13.526	26.084
A_2	[°C]	13.298	18.681	41.65	36.836	21.676	13.362
A_3	[°C]	17.346	-	-	-	-	-
$\sum (A_1+A_2+A_3)$ or $\sum (A_1+A_2)$	[°C]	38.3373	31.456	63.73	49.374	35.202	39.446
w_1	[°C]	1.9436	3.1794	2.3134	2.5146	2.363	5.0376
w_2	[°C]	11.531	8.067	12.07	6.605	7.179	1.84
w_3	[°C]	4.2645					
T_{c1}	[°C]	-51.335	-54.065	-51.768	2.4778	2.201	13.456
T_{c2}	[°C]	-51.518	-58.987	-47.724	17.159	10.944	2.2629
T_{c3}	[°C]	-51.83					
T_{o1}	[°C]	1.1218	1.7279	3.2578	2.4778	2.201	13.456
T_{o2}	[°C]	7.9628	12.154	16.189	17.159	10.944	2.2629
T_{o3}	[°C]	2.5736					
SD^2	[-]	0.00003	0.00014	0.00071	0.00139	0.00021	0.00017
R^2	[-]	0.99989	0.99921	0.99844	0.9957	0.99915	0.99949

8 Conclusions

HTPB and GAP based binders were prepared with different isocyanates and different plasticizers. DMA was used to analyze the cured elastomeric binders to understand the effect of isocyanates on the molecular transitions of the polymeric network. Use of different plasticizer allowed to see their effect in reducing the glass-rubber transition of HTPB+IPDI polyurethane networks. Evolution of the loss factor curves as a function of measurement temperature showed distinct differences in the intensity of loss factor curves with different isocyanates in the following order HDI > IPDI >> 6HMDI > Desmodur™ E305.

Two different curing agents Desmodur™ N100 and Desmodur™ N3400 showed differences in the trend of tanδ curves obtained with GAP polymers. N100 provided lower glass-rubber transition, whereas N3400 provided more flexibility or molecular mobility to the GAP network, when Bu-NENA was used as a plasticizer. Bu-NENA resulted in lower glass-rubber transition compared to the analogous formulation with BDNPF/A. On the other hand, BDNPF/A exerts less restriction on the mobility in the polymeric network as the intensity of this binder formulation is higher than that having Bu-NENA. Considering the area under the curves, indeed the sample with Bu-NENA (TS-11XG) resulted in a higher intensity value compared to BDNPF/A (TS-14XG), which makes it a better plasticizer for GAP systems. BDNPF/A which is a hydrophilic substance was not easy to incorporate in the GAP network as it is prone to catch undesired moisture within itself, which was the case during this study as well. The lowest Tg region was obtained with BATEG, but its tensile properties should be increased in order to be used it in any full formulation.

Loss factor curves collected from DMA were first corrected with BLC technique and the resulting data were further analyzed with EMG modelling quantitatively. Modelling of the loss factor curves with a suitable EMG function provide quantitative data of the transition regions (molecular mobility of chain elements), which enables to compare certain binder and/or filled composite propellant structures. In the development of a binder network and/or a new propellant formulation, EMG modelling of DMA data enables one to have an preview of the effect of new components used in the formulation, which reduces the amount of experimental trials.

9 Acknowledgments

The Scientific and Technological Research Council of Turkey (TÜBITAK) providing the 2219-International Post-Doctoral Research Programme is greatly acknowledged for the support of the first author (TS). First author would like to thank Dr. M.A. Bohn for collaboration on the research proposal. Energetic Materials Department of Fraunhofer ICT is greatly acknowledged for the possibility to perform there the research work. Mr. F. Ratzel and Mr. S. Fischer are thanked for the help to get acquaintance to the process laboratory in Fraunhofer ICT. Roketsan Missiles Industries, Ankara, Turkey is greatly acknowledged for the permission for post-doctoral research in Fraunhofer ICT for the first author (TS).

10 Abbreviations

ARES	: Advanced Rheometric Expansion System
ADN	: Ammonium dinitramide
BATEG	:bis-azido trietehylene glycol also triethylene glycol diazide (TEGDN)
BLC	: Base Line Correction of loss factor
BDNPA	: Bis-(2,2-dinitro-propyl)-acetal
BDNPF	: bis-(2,2-dinitro-propyl)-formal
Bu-NENA	: Butyl Nitroxy ethyl nitramine
SCRP	: Solid composite rocket propellant
DE™305	: Desmodur™ E305
DOS	: Dioctyl sebacate (plasticizer)
DOZ	: Dioctyl azelate (plasticizer)
DOA	: Dioctyl adipate (plasticizer)

DSC : Differential Scanning Calorimetry
DMA : Dynamic Mechanical Analysis
GAP : Glycidyl azide polymer
HDI : Hexamethylene diisocyanate (isocyanate)
HTPB : Hydroxyl Terminated PolyButadiene (here the type HTPB R45 HTLO)
IDP : Isodecyl pelargonate (plasticizer)
IPDI : Isophorone diisocyanate (isocyanate), has four conformation isomers
6HMDI : 4,4′-Methylene-bis-(cyclohexyl isocyanate), three conformation isomers also named H12MDI, also Desmodur^{TM} W
MDI : 4,4′-Methylene-bis-(phenyl isocyanate)
2-NDPA : 2 – nitro-diphenylamine
NCO : Isocyanate group
OH : Hydroxyl groups
Req : equivalent ratio, Req = NCO/OH
EMG : Exponentially modified Gauss distribution
tanδ : Loss factor (loss tangent); characterisation of the glass-rubber transition in elastomers or in polymers; tanδ = G''/G' = E''/E'
G' : Storage shear modulus
G'' : Loss shear modulus
G* : complex shear modulus, G* = G' +iG'', $|G^*| = \sqrt{G'^2 + G''^2}$
δ : Phase angle, angle between stress and strain in the dynamical measurement
Tg : Glass-rubber transition temperature, here defined as maximum of the loss factor curve in DMA measurements, $T_{g,DMA}$

11 References

[1] Cerri, S., Bohn, M.A., Separation of Molecular Mobility Ranges in Loss Factor Curves by Modelling with Exponentially Modified Gauss Distributions, *Paper 87, pages 87-1 to 87-16 in Proceed. of 41th International Annual Conference of ICT on 'Energetic Materials,* Karlsruhe, Germany, June 29 to July 2, 2010.

[2] Bohn, M.A., Cerri, S., Molecular mobility in binder systems, pages 96-1 to 96-33 in *Proceedings of the 42nd International Annual Conference of ICT on 'Energetic Materials – Modelling, Simulation and Characterisation of Pyrotechnics, Propellants and Explosives'*, Karlsruhe, Germany, June 28 to July 1, 2011.

[3] Bohn, M.A., Modeling of loss factors of elastomer binders for high explosive charges and composite rocket propellants to separate binder fractions with different molecular mobility used to follow aging, paper 118 on the *10th International Symposium on Special Topics (ISICP) in Chemical Propulsion & Energetic Materials*, Poitiers, France, 2-6 June 2014.

[4] Cerri S., Bohn, M.A., Menke, K., Galfetti, L., Aging of HTPB/Al/AP Rocket Propellant Formulations Investigated by DMA Measurements, *Propellants Explos. Pyrotech.* 38, p. 190-198, 2013.

[5] Cerri, S., Characterisation of the Ageing of Advanced Solid Rocket Propellants and First Step Design of Green Propellants, PhD Thesis, Politecnico di Milano, Dipartimento di Energia, Dottorato di Ricerca in Energetica, XXII Ciclo, 2011.

[6] Bohn, M.A., Mußbach, G., Cerri, S. Influences on the loss factor of elastomer binders and its modelling, Paper 60, pages 60-1 to 60-43 in *Proceedings of the 43rd Int. Ann. Conf. of ICT Karlsruhe, Germany, June 26 to 29,* 2012.

[7] Niklas Wingborg, Increasing the tensile strength of HTPB with different isocyanates and chain extenders, Polymer Testing, Volume 21, Issue 3, 2002, Pages 283-287, ISSN 0142-9418, http://dx.doi.org/10.1016/S0142-9418(01)00083-6.

[8] Eroglu, Mehmet S. Characterization of the network structure of hydroxyl terminated poly (butadiene) elastomers prepared by different reactive systems.Journal of applied polymer science, 1998, 70.6: 1129-1135.

[9] Bina, C. Korah, K. G. Kannan, and K. N. Ninan. "DSC study on the effect of isocyanates and catalysts on the HTPB cure reaction." Journal of thermal analysis and calorimetry 78.3 (2004): 753-760.

[10] V Sekkar, S Venkatachalam, K.N Ninan, Rheokinetic studies on the formation of urethane networks based on hydroxyl terminated polybutadiene, European Polymer Journal, Volume 38, Issue 1, January 2002, Pages 169-178.

[11] Muthiah, Rm, et al. "Energetics and compatibility of plasticizers in composite solid propellants." Defence Science Journal 39.2 (2013): 147-155.
[12] Tor Erik Kristensen, Tomas Lunde Jensen, Erik Unneberg, Development of Smokeless Nitramine Composite Rocket Propellants at FFI and NAMMO, Paper 7 in Proceedings of the 45th Int. Ann. Conf. of ICT Karlsruhe, Germany.
[13] Volker Gettwert, Andrea Franzin, Manfred A. Bohn, Luigi T. DeLuca, Thomas Heintz, and Volker Weiser, ADN/GAP COMPOSITE propellants with and without metallic fuels, *10th International Symposium on Special Topics (ISICP) in Chemical Propulsion & Energetic Materials*, Poitiers, France, 2-6 June 2014.
[14] Smokeless Composite Propellants Based on HMX/GAP/BuNENA, Thomas Deschner, Eirik André Løkke, 92, 7 in Proceedings of the 45th Int. Ann. Conf. of ICT Karlsruhe, Germany..
[15] Origin Version 7.0 (German), SR 4, v7.0552, Data Analysis and Graphing Software, OriginLab Corporation, Round House Plaza, Northhampton, MA 01060, USA.
[16] Viswanadhan, V. N., Ghose, A. K., Revankar, G. R., Robins, R. K., Atomic physicochemical parameters for three dimensional structure directed quantitative structure-activity relationships, *J. Chem. Inf. Comput. Sci.,* 29, 163-172**,** 1989.
[17] Technical Data Sheet Bayer Materials, Desmodur™ E305.
[18] Rhein, R.A. (1983) Energetic Polymers and Plasticizers , Naval Weapons Center, China Lake , NWC TP 6410. References 323.
[19] Provatas, A. (2000) Energetic Polymers and Plasticizers for Explosive Formulations: A Review of Recent Advances . AAMRL, Australia, Report No. DSTO - TR-0966.
[20] Hammel , E.E. (1982) Research on polynitroaliphatics for use in solid propellants . 13th Intl Ann. Conf. ICT, Karlshrue, Germany, June 30 – July 2, 1982 , p. 69.
[21] http://nptel.ac.in/courses/116102006/11.
[22] Adam, N., Avar, G., Blankenheim, H., Friederichs, W., Giersig, M., Weigand, E., Halfmann, M., Wittbecker, F.-W., Larimer, D.-R., Maier, U., Meyer-Ahrens, S., Noble, K.-L. and Wussow, H.-G. 2005. Polyurethanes. Ullmann's Encyclopedia of Industrial Chemistry. .
[23] Jai Prakash Agrawal, High Energy Materials: Propellants, Explosives and Pyrotechnics, Wiley-VCH, Weinheim, 2010.
[24] Cerri, S., Bohn, M. A., Menke, K. and Galfetti, L. (2014), Aging of ADN Rocket Propellant Formulations with Desmophen®-Based Elastomer Binder. Propellants, Explosives, Pyrotechnics, 39: 526–537. doi: 10.1002/prep.201300124